



ELSEVIER

Journal of Alloys and Compounds 330–332 (2002) 271–275

Journal of
ALLOYS
AND COMPOUNDS

www.elsevier.com/locate/jallcom

Degradation behavior of $\text{LaNi}_{5-x}\text{Sn}_x\text{H}_z$ ($x=0.20-0.25$) at elevated temperatures

R.C. Bowman Jr.^{a,*}, C.A. Lindensmith^a, S. Luo^b, Ted B. Flanagan^b, T. Vogt^c^aJet Propulsion Laboratory, California Institute of Technology, 4800 Oak Grove Dr., Pasadena, CA 91109-8099, USA^bDepartment of Chemistry, University of Vermont, Burlington, VT 05405, USA^cDepartment of Physics, Brookhaven National Laboratory, Upton, NY 11973-5000, USA

Abstract

Systematic studies of the hydriding behavior of $\text{LaNi}_{5-x}\text{Sn}_x$ alloys with tin contents in the range $0.20 < x < 0.25$ have revealed changes in the pressure–composition–temperature (P – C – T) isotherms measured after heating the hydrides above 450 K. Some loss in reversible capacity was observed along with reductions in the plateau pressures and hysteresis ratios while the slopes of the plateaus became greater. These changes are indications of degradation processes and increased disorder within the alloy structure. Additional experiments were performed for long periods (i.e. >1000 h) at elevated temperatures and hydrogen pressure to produce further degradation in the P – C – T isotherms. The impact of alloy composition on the isotherms has been determined. The crystal lattice properties of the alloys before and after hydrogen reactions have been studied using high-resolution X-ray powder diffraction with synchrotron radiation. Changes in these X-ray diffraction patterns are correlated to various structural modifications resulting from hydride formation and degradation. © 2002 Elsevier Science B.V. All rights reserved.

Keywords: La–Ni–Sn alloys; CaCu_5 phases; P – C isotherms; Non-stoichiometric alloys; Hydride degradation behavior; X-ray diffraction

1. Introduction

Tin (Sn) substitution for a portion of the nickel in LaNi_5 has been shown [1,2] to alter many of the thermodynamic properties of the resulting hydride phase as evident from the P – C – T isotherms for these alloys. Namely, Sn reduces the plateau pressures, hydrogen storage capacity, and hysteresis ratio while the enthalpy of formation for the hydride phase becomes more exothermic [1]. Sn levels as small as $x=0.05$ have been found [3] to prevent formation of the intermediate γ -phase in LaNi_5H_z and accompanying splitting of the plateau for $T > 350$ K. Furthermore, Sn also significantly enhances the stability of the hydride during both temperature cycling [4] under hydrogen gas and electrochemical cycling [5]. Although a complete explanation on how Sn makes the $\text{LaNi}_{5-x}\text{Sn}_x\text{H}_z$ system more robust to degradation has not been established, stronger chemical bonding of Sn to La and Ni is believed [6] to

inhibit metal atom diffusion and defect/dislocation formation in the hydride.

Amongst several promising applications of the Sn substituted alloys, their use in the compressors for closed-cycle, Joule–Thomson (J–T) sorption cryocoolers is especially attractive for long-life space missions [7–9]. Desirable characteristics from the sorbent hydrides in these cryocoolers include broad and flat plateaus with minimum hysteresis as well as little degradation in either reversible hydrogen storage capacity or shapes of the isotherms during many thousands of cycles from 270–300 to 450–525 K. To satisfy the demanding performance necessary for some space missions [8,9], alloy properties need to be optimized for power efficiency, cooling temperature range and heat load, and stability during multiple year flights.

Many factors influence the hydriding properties of the AB_5 alloys, but alloy composition and stoichiometry are probably the most important. In particular, B/A ratios > 5.0 produce pressure increases, larger plateau slopes, and diminished capacities for AB_5 alloys [10,11]. The excess B atoms are accommodated in the crystal structure by B_2 -dumbbells randomly substituting at La sites [12]. This behavior has been previously observed for $\text{La}(\text{Ni},\text{Sn})_{5+y}$ alloys [13], but the impact on thermodynamic properties

*Corresponding author. Tel.: +1-818-374-7941; fax: +1-818-393-4878.

E-mail address: robert.c.bowman-jr@jpl.nasa.gov (R.C. Bowman Jr.).

has not been thoroughly evaluated. The present paper reports systematic characterization of the P – C – T isotherms for Sn substituted alloys in the range of $0.20 < x < 0.25$ for variation of the (Ni+Sn)/La ratios from 4.96 to 5.18 and different purity levels of the La metal. Differences were noted not only in the initial plateau pressures after activation, but also in the influence of elevated temperature (i.e. $T > 450$ K) on degradation induced changes in the isotherms.

2. Experimental details

The nominal $\text{LaNi}_{5-x}\text{Sn}_x$ alloys with $0.20 < x < 0.25$ were produced by either arc-melting or induction melting followed by annealing under purified argon at 1223 K for 100–120 h as described previously [2–4]. All alloys were examined by optical metallography, powder X-ray diffraction (XRD) using Cu $K\alpha$ radiation, elemental and electron microprobe analyses. Alloy compositions and crystal lattice properties are summarized in Table 1. Isotherms were measured by conventional volumetric techniques on one of two all-metal Sieverts' systems. Most isotherm data were obtained at the University of Vermont on previously described [1–3] equipment. A computer controlled apparatus utilizing an oil-free vacuum pumping station, electropolished 316L stainless steel components, and point-of-use filtration (MilliPore Corporation, Bedford, MA, USA) to purify further the research-grade hydrogen gas was used at the Jet Propulsion Laboratory (JPL) for isotherm determinations and long duration (> 1000 h) treatment at high temperatures ($T > 460$ K) and hydrogen pressure ($P > 150$ bar). The two systems gave indistinguishable P – C – T results for samples of the same alloy.

The high-resolution XRD patterns were obtained at the National Synchrotron Light Source at the Brookhaven National Laboratory as described elsewhere [13].

3. Results and discussion

The properties for ten alloys are given in Table 1. While several alloys are nearly exactly stoichiometric (i.e. $\{\text{Ni} + \text{Sn}\}/\text{La} = 5.00$), others (i.e. samples Sn20–MPC551, Sn22–BPC872, and Sn25–MPC1860) have $\{\text{Ni} + \text{Sn}\}/\text{La} > 5.0$. There is an interesting increase in the c/a ratio from ~ 0.795 to 0.800 for these latter alloys which agrees with behavior of the lattice parameters for other non-stoichiometric AB_{5+x} alloys [10–13]. Although the unit cell volume increases with additional Sn substitution [14,15], the volumes are slightly smaller in Table 1 for nominally identical Sn content when $\{\text{Ni} + \text{Sn}\}/\text{La} > 5.0$. Although most alloys were found to be single phase after heat treatment at 1223 K, two (i.e. Sn25–HCI and Sn–AGR51) contained a small amount of the intermetallic LaNiSn phase [15] which reduces the proportion of Sn in the main $\text{La}(\text{Ni},\text{Sn})_{5+y}$ phase and thus impacts the isotherms.

Hydrogen absorption and desorption isotherms measured at 373 K for several $\text{Sn} = 0.20$ – 0.25 alloys are presented in Fig. 1 and 300 K isotherms for nominal $\text{Sn} = 0.22$ alloys are shown in Fig. 2. These results were obtained after activation [14] and completion of several isotherms at $T = 373$ K and lower temperatures, but to avoid possible degradation the hydride phase was not formed above 373 K. Although it is well-established [1,14,15] that increasing the Sn content leads to expansion of the cell volume and a decrease in plateau pressure, Fig. 1 clearly demonstrates that the pressures for the non-stoichiometric alloys Sn20–MPC551 and Sn25–MPC1860 exceed the pressures obtained for the $x = 0.20$ alloy Sn20–Ref. The isotherms for Sn25–MPC1860 are also significantly greater than pressures for the other three nearly stoichiometric $\text{Sn} = 0.25$ alloys. Furthermore, Sn20–MPC551 and Sn25–MPC1860 have larger slopes across the plateau region and reduced storage capacities. These features are typical for other non-stoichiometric LaB_{5+y} alloys [10,11]. The lowest pressures and least plateau slopes among the $\text{Sn} = 0.25$

Table 1

Properties of $\text{LaNi}_{5-x}\text{Sn}_x$ alloys including lattice parameters (a , c) and hydrogen absorption (P_{abs})/desorption (P_{des}) pressures measured in plateau region ($\text{H}/\text{La}(\text{Ni},\text{Sn})_{5+y} = 2.0$)

Sample ID	Alloy composition	La purity (at%)	a (nm)	c (nm)	c/a	Volume ($\text{nm}^3 \cdot 10^{-3}$)	Inclusions (wt%)	300 K $P_{\text{abs}}/P_{\text{des}}$ (kPa)
Sn20–Ref	$\text{LaNi}_{4.86}\text{Sn}_{0.20}$	99.95	0.50516 ^a	0.40098 ^a	0.7953	88.62	None	56.2/47.9 ^b
Sn20–MPC551	$\text{LaNi}_{4.96}\text{Sn}_{0.21}$	NA	0.50433	0.40249	0.7981	88.66	None	89.1/72.4
Sn22–BPC872	$\text{LaNi}_{4.87}\text{Sn}_{0.22}$	99.91	0.50512	0.40277	0.7974	89.01	None	61.7/56.5
Sn22–AGR278	$\text{LaNi}_{4.74}\text{Sn}_{0.22}$	99.91	0.50587	0.40230	0.7953	89.16	None	45.0/39.7
Sn22–AGR280	$\text{LaNi}_{4.77}\text{Sn}_{0.23}$	99.25	0.50577	0.40257	0.7960	89.18	None	50.7/43.6
Sn22–AGR281	$\text{LaNi}_{4.77}\text{Sn}_{0.23}$	98.07	0.50568	0.40251	0.7960	89.14	None	50.5/43.3
Sn25–HCI	$\text{LaNi}_{4.75}\text{Sn}_{0.25}$	NA	0.50625	0.40386	0.7945	89.27	LaNiSn ($\sim 1\%$)	40.7/32.4
Sn25–MPC1860	$\text{LaNi}_{4.91}\text{Sn}_{0.27}$	99.87	0.50439	0.40386	0.8007	88.98	None	72.4/64.6
Sn25–AGR50	$\text{LaNi}_{4.75}\text{Sn}_{0.25}$	99.80	0.50651	0.40269	0.7950	89.47	None	33.1/30.2
Sn25–AGR51	$\text{La}_{1.02}\text{Ni}_{4.75}\text{Sn}_{0.25}$	99.80	0.50629	0.40217	0.7948	89.18	LaNiSn ($\sim 2\%$)	45.2/38.0

^a Lattice parameters previously determined — from Ref. [3].

^b Isotherm previously measured at 298 K [2].

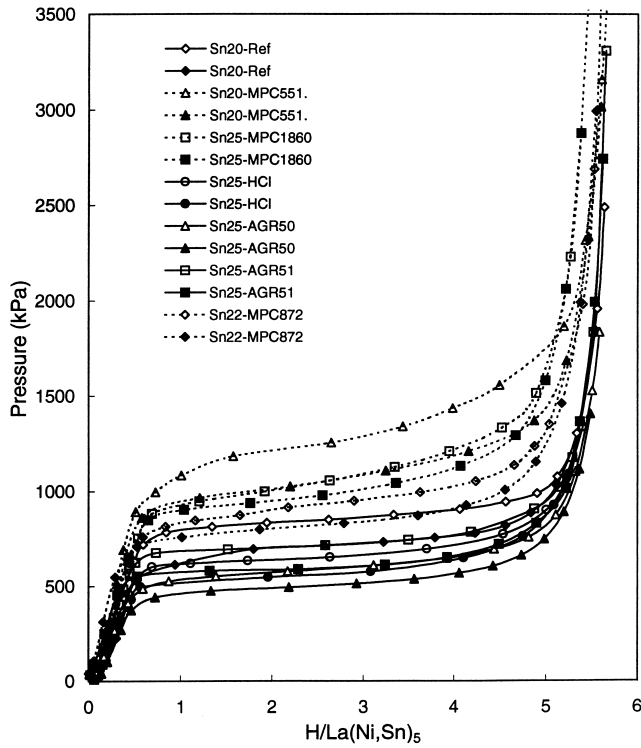


Fig. 1. Hydrogen isotherms for $\text{LaNi}_{5-x}\text{Sn}_x$ ($x=0.20\text{--}0.25$) alloys at 373 K. Open symbols represent absorption while filled symbols desorption.

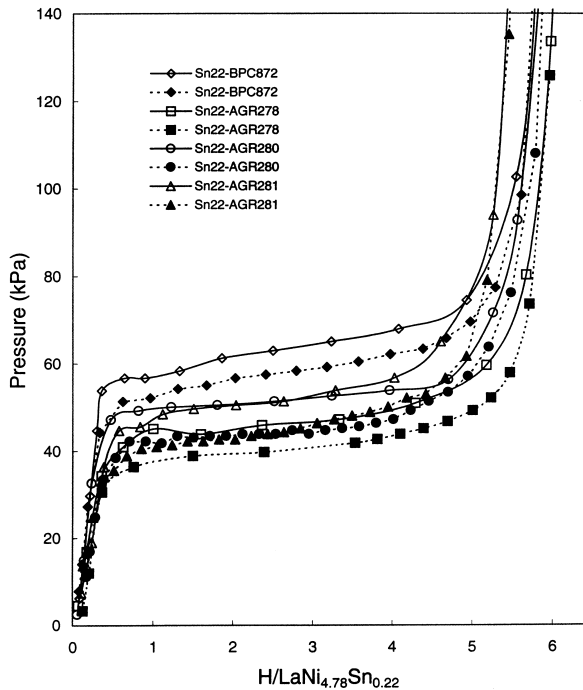


Fig. 2. Hydrogen isotherms for $\text{LaNi}_{4.78}\text{Sn}_{0.22}$ alloys at 300 K. Open symbols and solid lines represent absorption while filled symbols and dashed lines desorption.

alloys was for the single phase Sn25–AGR50 material where presumably the Sn distribution is most uniform. In Fig. 2 the non-stoichiometric alloy Sn22–BPC872 has the highest pressures and greatest plateau slopes for the Sn = 0.22 alloys. However, the difference is not so large as the deviation of the $(\text{Ni} + \text{Sn})/\text{La}$ ratio from 5.0 is less which is also consistent with the smaller increase in the c/a ratio for Sn22–BPC872 reported in Table 1. The results for Sn22–AGR281 (Fig. 2) also show that La metal purity impacts the isotherms mainly through reduced capacity and slightly higher pressures compared to Sn22–AGR278 made with the purer La. All of the effects discussed for Figs. 1 and 2 were observed for isotherms obtained at other temperatures.

Although Sn definitely reduces disproportionation of $\text{LaNi}_{5-x}\text{Sn}_x\text{H}_z$ phases [4], some degradation at elevated temperatures has been noted. Fig. 3 shows the impact of relatively short treatments at $T=493$ K and pressures above 125 bar on the post-aging 300 K isotherms for two Sn = 0.22 alloys. While both systems experience downward shifts in plateau pressure and increased slopes with aging, the changes are greater for the non-stoichiometric alloy Sn22–BPC872. When hydrides of two nominally stoichiometric Sn = 0.25 alloys were aged at higher temperature and longer duration, more moderate changes were found as shown in Fig. 4. Apparently, the greater disorder in the non-stoichiometric alloys does enhance the degradation process beyond that occurring in the ideal AB_5 composition. One of the challenges is to identify the responsible mechanism.

As described by Sandrock et al. [16], disproportionation

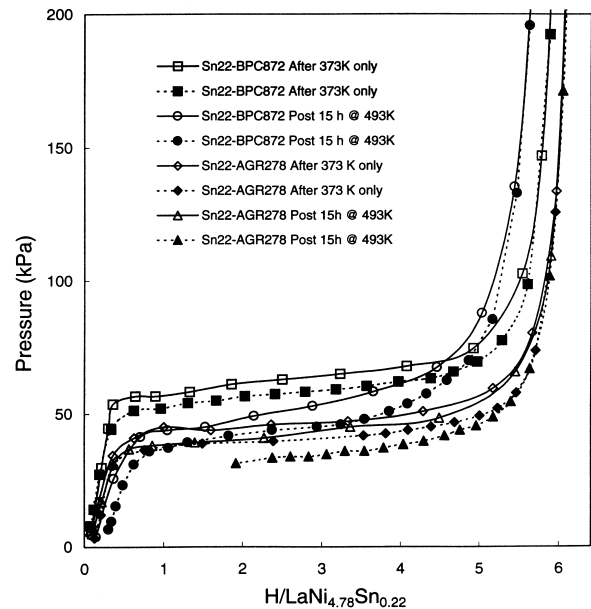


Fig. 3. Hydrogen isotherms for $\text{LaNi}_{4.78}\text{Sn}_{0.22}$ alloys at 300 K before and after aging at 493 K. Open symbols and solid lines represent absorption while filled symbols and dashed lines desorption.

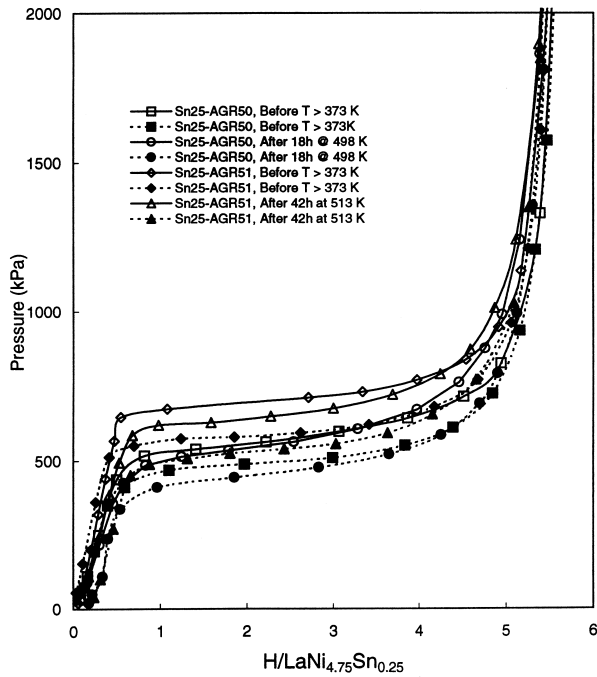


Fig. 4. Hydrogen isotherms for $\text{LaNi}_{4.75}\text{Sn}_{0.25}$ alloys at 373 K before and after aging at $T > 495$ K. Open symbols and solid lines represent absorption while filled symbols and dashed lines desorption.

of LaNi_5 hydrides can be produced by accelerated aging at high temperatures. Several samples of the Sn22–BPC872 alloy have been subjected to aging at temperatures above 460 K and pressures over 140 bar at hydride contents greater than $z = 5.0$. These conditions should maximize any degradation since the material will be entirely β -phase for this composition. The extent of degradation was found to increase as the aging temperature was raised. Fig. 5 shows the impact of aging at 473 K for 1425 h on desorption isotherms at 373 K and above. Aging produced loss in reversible hydrogen storage capacity, downward shift in plateau pressure, and large increase in the slope. Similar effects were seen in absorption and desorption isotherms measured at lower temperature. The extensive degradation produced by 1125 h aging at 485 K is shown in Fig. 6 to be removed by a regeneration treatment of ~ 15 h at 673 K under dynamic vacuum.

Cerny et al. [17] recently indicated that comparisons of the unit cell parameters for a variety of hydrogen cycled and non-cycled AB_{5+y} samples often yield an a axis decrease while the c axis expands to leave the unit cell volume nearly constant. However, the one tin substituted alloy that Cerny et al. had examined (i.e. $\text{LaNi}_{4.5}\text{Sn}_{0.5}$) showed an increase of both a and c . Using high-resolution XRD, we have observed a range of different responses of the unit cell parameters upon cycling that cannot be generalized in such a simple and straightforward mechanism. These results indicate that a far more complex microstructure evolves along with the changes in P – C – T isotherms at elevated temperatures.

For a Sn22–BPC872 sample which underwent just two

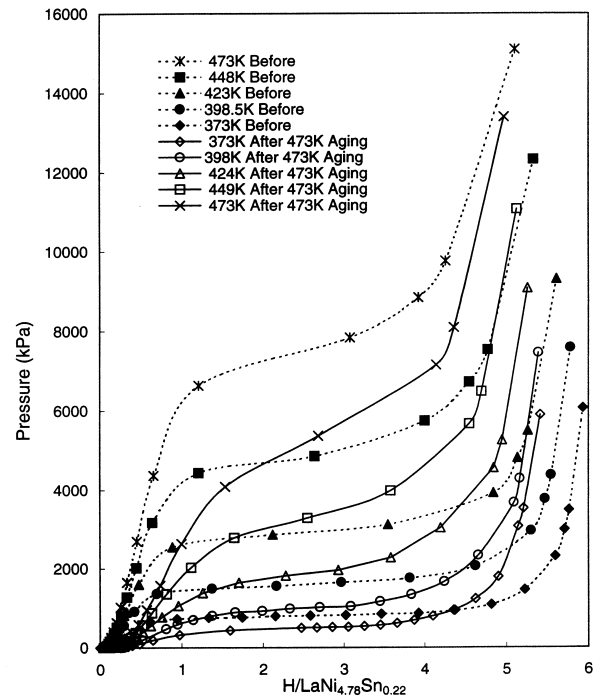


Fig. 5. Desorption isotherms for $\text{LaNi}_{4.78}\text{Sn}_{0.22}\text{H}_2$ alloy Sn22–BPC872 before (open symbols and solid lines) and after 1425 h at 473 K aging (filled symbols and dashed line) with pressure > 139 bar and initial $z = 5.29$.

373 K and one 300 K hydrogen cycling processes, the a axis decreased from 0.505291(8) to 0.505207(4) nm; whereas the c axis remains constant (i.e. 0.402894(22) to

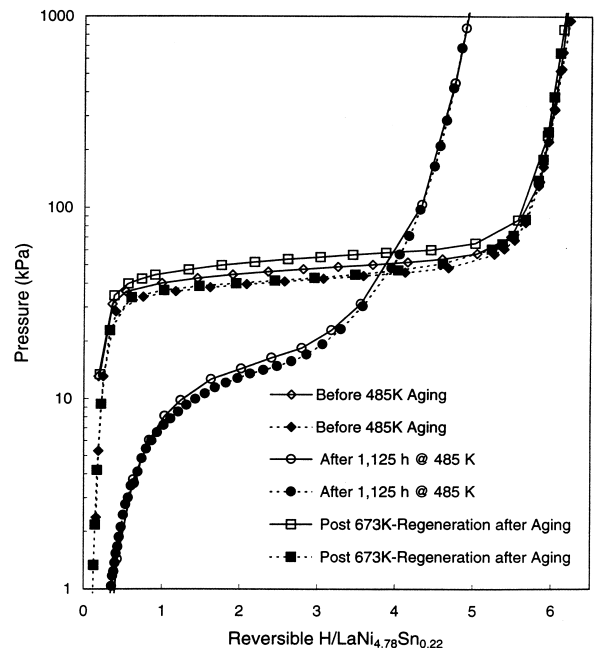


Fig. 6. Hydrogen isotherms at 300 K for $\text{LaNi}_{4.78}\text{Sn}_{0.22}\text{H}_2$ alloy Sn22–BPC872 before aging, after 1125 h aging at 485 K with pressure > 171 bar and initial $z = 5.10$, and vacuum regeneration at 673 K after aging. Open symbols and solid lines represent absorption while filled symbols and dashed lines desorption.

0.402895(14) nm) compared to the unreacted alloy. However, another Sn22–BPC872 sample that was used for 18 hydriding cycles at various temperatures up to $T=493$ K and also exhibited the downward shift in plateau pressures (Fig. 3) had increases of both a and c axes to 0.505619(13) and 0.403229(29) nm, respectively. Williamson–Hall analyses [18] of the XRD peak widths were used to determine the mean crystallite size L and distribution of the d -spacings $\Delta d/d$ for these samples. It was found that the compositional fluctuations, which were extracted from the slopes after correcting for the instrumental contributions, remain constant after initial hydriding cycles. However, the significant line broadening of the $\langle 00l \rangle$ reflections indicated the ‘correlation length’ along the c -axis decreases from ~ 350 to ~ 150 nm. For the alloy that was cycled more times and up to $T=493$ K, this correlation length remains constant along with the compositional fluctuation, but there were increases for both a and c axes. This behavior could be indicative of the interplay between first- and second-type effects as discussed by Krivoglaz [19]. First-type effects such as dislocation loops, dipoles, vacancies and interstitials change the lattice parameters but result in no line broadening; whereas, second-type defects such as dislocations induce line broadening but no change of lattice parameters. It appears that both types are occurring at different stages of the hydriding–dehydriding processes for these $\text{La}(\text{Ni},\text{Sn})_{5+y}$ alloys.

High-resolution XRD parameters were also obtained for the two $\text{Sn}=0.25$ alloys whose isotherms are given in Fig. 4 before and after cycling to $T>495$ K. The Sn25–AGR50 samples indicate the similar increase of the a and c unit cell parameters upon hydriding as seen for the $\text{Sn}=0.22$ alloy while the slope of the Williamson–Hall plots indicates that the strain inferred from the $\Delta d/d$ variations remains constant within the errors. The Sn25–AGR51 alloys show another type of response to hydriding: the a unit cell parameter increases while the c parameter decreases upon hydriding. The role of the secondary phase for this latter sample is unclear and needs more study. The distinct and complex behavior of tin-substituted $\text{La}(\text{Ni},\text{Sn})_{5+y}$ alloys indicates that various mechanisms are probably involved for the different stages of activation, absorption, desorption, and degradation at elevated temperatures. More comprehensive investigations are needed to link the structural response with the changes observed in the P – C – T diagrams. Further work along these lines is in progress and will be reported at a later date.

4. Conclusions

Deviations in the stoichiometry of $\text{La}(\text{Ni},\text{Sn})_{5+y}$ alloys not only produce changes in hydrogen isotherms similar to those described for other LaNi_5 -based hydrides [10,11] but their hydrides are also more vulnerable to the reversible degradation effects at elevated temperature. When less pure

La metal is used to make the alloys, the hydrogen isotherms exhibit changes consistent with $(\text{Ni}+\text{Sn})/\text{La}>5.0$. Nevertheless, $\text{LaNi}_{5-x}\text{Sn}_x\text{H}_z$ with $x=0.20$ – 0.25 is much more resistant to disproportionation reactions at $T>350$ K than nearly all other AB_5 hydrides. Consequently, these alloys are the leading candidates for demanding applications such as use in the compressors of hydrogen sorption cryocoolers for space missions [7–9].

Acknowledgements

This research was carried out by the Jet Propulsion Laboratory, California Institute of Technology, under a contract with the National Aeronautical and Space Administration. Authors thank T.M. Riedemann and his colleagues at Ames Laboratory for preparation and chemical analyses of the alloys. J.G. Kulleck performed the powder XRD measurements at JPL.

References

- [1] S. Luo, W. Luo, J.D. Clewley, T.B. Flanagan, L.A. Wade, J. Alloys Comp. 231 (1995) 467.
- [2] S. Luo, W. Luo, J.D. Clewley, T.B. Flanagan, R.C. Bowman Jr., J. Alloys Comp. 231 (1995) 473.
- [3] S. Luo, J.D. Clewley, T.B. Flanagan, R.C. Bowman Jr., J.S. Cantrell, J. Alloys Comp. 253–254 (1997) 226.
- [4] R.C. Bowman Jr., C.H. Luo, C.C. Ahn, C.K. Witham, B. Fultz, J. Alloys Comp. 217 (1995) 185.
- [5] B.V. Ratnakumar, C. Witham, R.C. Bowman Jr., A. Hightower, B. Fultz, J. Electrochem. Soc. 143 (1996) 2578.
- [6] R.V. Bugga, G. Halpert, B. Fultz, C.K. Witham, R.C. Bowman Jr., A. Hightower, US Patent No. 5,656,388, issued August 12, 1997.
- [7] B.D. Freeman, E.L. Ryba, R.C. Bowman Jr., J.R. Phillips, Int. J. Hydrogen Energy 22 (1997) 1125.
- [8] P. Bhandari, R.C. Bowman Jr., R.G. Chave, C.A. Lindensmith, G. Morgante, C. Paine, M. Prina, L.A. Wade, Astrophys. Lett. Commun. 37 (2000) 227.
- [9] L.A. Wade, P. Bhandari, R.C. Bowman Jr., C. Paine, G. Morgante, C.A. Lindensmith, D. Crumb, M. Prina, R. Sugimura, D. Rapp, Adv. Cryogenic Eng. 45 (2000) 499.
- [10] K.H.J. Buschow, H.H. van Mal, J. Less-Common Metals 29 (1972) 203.
- [11] S. Luo, T.B. Flanagan, P.H.L. Notten, J. Alloys Comp. 239 (1996) 214.
- [12] W. Coene, P.H.L. Notten, F. Hakkens, R.E.F. Einerhand, J.L.C. Daams, Philos. Mag. A 65 (1992) 1485.
- [13] T. Vogt, J.J. Reilly, J.R. Johnson, G.D. Adzic, J. McBreen, Electrochem. Solid-State Lett. 2 (1999) 111.
- [14] S. Luo, J.D. Clewley, T.B. Flanagan, R.C. Bowman Jr., L.A. Wade, J. Alloys Comp. 267 (1998) 171.
- [15] J.-M. Joubert, M. Latroche, R. Cerny, R.C. Bowman Jr., A. Percheron-Guegan, K. Yvon, J. Alloys Comp. 293–295 (1999) 124.
- [16] G.D. Sandrock, P.D. Goodell, E.L. Huston, P.M. Golden, Z. Phys. Chem. NF164 (1989) 1285.
- [17] R. Cerny, J.-M. Joubert, M. Latroche, A. Percheron-Guegan, K. Yvon, J. Appl. Crystallogr. 33 (2000) 997.
- [18] G. K. Williamson, W.H. Hall, Acta Metall. 1 (1953) 22.
- [19] M.A. Krivoglaz, Theory of X-ray and Thermal Neutron Scattering by Real Crystals, Plenum Press, New York, 1969.